

# A theoretical approach to predict the performance of chevron-type plate heat exchangers

Holger Martin

*Thermische Verfahrenstechnik, Universität Karlsruhe (TH), D-76128 Karlsruhe, Germany*

Received 18 September 1995; accepted 6 October 1995

## Abstract

Manufacturers of plate and frame heat exchangers nowadays mainly offer plates with chevron (or herringbone) corrugation patterns. The inclination angle  $\varphi$  of the crests and furrows of that sinusoidal pattern relative to the main flow direction has been shown to be the most important design parameter with respect to fluid friction and heat transfer. Two kinds of flow may exist in the gap between two plates (pressed together with the chevron pattern of the second plate turned into the opposite direction): the crossing flow of small substreams following the furrows of the first and the second plate, respectively, over the whole width of the corrugation pattern, dominating at lower inclination angles (lower pressure drop); and the wavy longitudinal flow between two vertical rows of contact points, prevailing at high  $\varphi$  angles (high pressure drop). The combined effects of the longer flow paths along the furrows, the crossing of the substreams, flow reversal at the edges of the chevron pattern, and the competition between crossing and longitudinal flow are taken into account to derive a relatively simple but physically reasonable equation for the friction factor  $\xi$  as a function of the angle  $\varphi$  and the Reynolds number  $Re$ . Heat-transfer coefficients are then obtained from a theoretical equation for developing thermal boundary layers in fully developed laminar or turbulent channel flow — the generalized L ev eque equation — predicting heat-transfer coefficients as being proportional to  $(\xi \cdot Re^2)^{1/3}$ . It is shown, by comparison, that this prediction is in good agreement with experimental observations quoted in the literature.

*Keywords:* Theoretical approach; Chevron-type plate heat exchangers; Performance prediction; Heat-transfer coefficients; Developing thermal boundary layers

## 1. Introduction

Plate and frame heat exchangers are offered by a large number of manufacturers as standard series production equipment over a wide range of sizes. They consist of a number of gasketed metal plates clamped between a stationary head and a follower plate by tie bolts. The principle, application and design characteristics of this very successful type of heat exchanger is explained in detail in relevant texts and handbooks [1–3]. Due to the great variety of possible corrugation patterns, and to the proprietary nature of the details of each particular design, the aim to provide users with reliable design equations for thermal and hydraulic performance of such equipment seemed to be hopeless. The fact, however, that during the last decades the chevron wave pattern had proved to be the most successful design offered in rather similar shapes by the majority of manufacturers has partly changed this situ-

ation. In the meantime, a number of detailed experimental studies, some of a more fundamental nature [4–7], using model corrugation patterns and systematically varying parameters like amplitude, wavelength, inclination angle and flow rate, and others with real industrial series heat exchangers [8–10], have produced a relatively large amount of interesting facts about heat transfer and pressure drop in plate heat exchangers. This wealth of detailed knowledge, however, has not yet been properly exploited to build up a generalized thermal and hydraulic design method for plate heat exchangers, comparable to the well-established methods for shell-and-tube heat exchangers. The following presents an entirely new approach to this problem: based on the very detailed experimental observations of Focke et al. [6] and Gaiser [7], the flow behaviour as known qualitatively from these sources is used to develop a relatively simple model to describe the effect of the inclination angle and the Reynolds number of fluid

friction. In turn, the heat transfer is calculated from a purely theoretical asymptotic equation for developing thermal boundary layers in fully developed laminar and turbulent channel flow — the generalized L ev eque equation — which so far has only been applied for laminar duct flow.

## 2. Fluid friction

The friction factor is defined as

$$\xi = \frac{2 \cdot \Delta p \cdot d_h}{\rho \cdot u^2 \cdot L_p} \quad (1)$$

( $\xi = 4f$ , where  $f$  is the Fanning friction factor, is also often used in the literature), where the hydraulic diameter  $d_h$  is defined as four times the fluid volume divided by the surface area, resulting in

$$d_h = 4\hat{a}/\Phi \quad (2)$$

where  $\hat{a}$  is the amplitude of the sinusoidal corrugation (see Fig. 1),  $2\hat{a}$  is the average gap width and the plate width between the gaskets ( $=4B$  in Fig. 1) is assumed to be much larger than  $2\hat{a}$ . The area enlargement factor  $\Phi$  is the ratio of the developed surface area to the projected area and depends on the ratio of amplitude  $\hat{a}$  to the wavelength (or pitch)  $\Lambda$ .

Using the dimensionless corrugation parameter

$$X = 2\pi\hat{a}/\Lambda \quad (3)$$

it can be calculated approximately for a sinusoidal corrugation from a three-point integration formula that

$$\Phi(X) \approx \frac{1}{6} (1 + \sqrt{1 + X^2} + 4\sqrt{1 + X^2/2}) \quad (4)$$

For  $\Lambda/\hat{a} = 2\pi$ ,  $X = 1$ ,  $\Phi \approx 1.22$ , a typical value of  $\Phi$  for technical corrugation patterns. To reach a surface enlargement of  $\Phi = 2$ , the ratio of wavelength to amplitude must be as small as  $\Lambda/\hat{a} = 2.46$ .

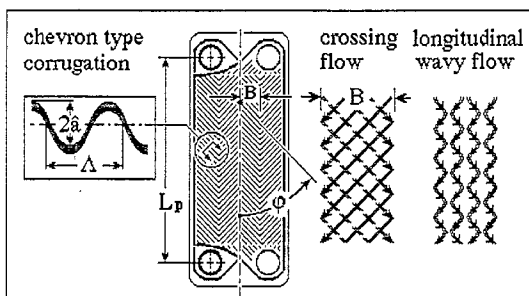


Fig. 1. Chevron-type heat exchanger plate, the angle  $\phi$  and the two flow patterns.

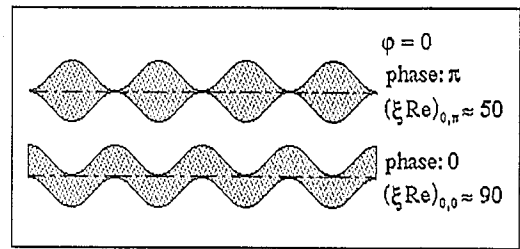


Fig. 2. Limiting cross-sections for  $\phi = 0^\circ$ , i.e. straight longitudinal duct flow, with the approximate values of the friction constants ( $\xi \cdot Re$ ) for laminar flow, (limiting longitudinal sections for  $\phi = 90^\circ$  corresponds to wavy longitudinal flow).

The vertical length of a plate,  $L_p$ , is usually measured between the centres of the upper and lower port holes (see Fig. 1), and  $u$  is the superficial velocity defined as the volumetric flow rate divided by the average flow cross-section (number of gaps of one side  $\times$  plate width between the gaskets  $\times 2\hat{a}$ ).

It should be mentioned that some authors use other definitions of hydraulic, or equivalent diameters, so, for example, the definition using the projection area rather than the developed area is often called the equivalent diameter

$$d_e = 4\hat{a} \quad (5)$$

The two definitions are therefore simply related by  $d_e = \Phi d_h$ .

From the experimental observations of Focke et al. [6] and Gaiser [7], it has become obvious that two kinds of flow do occur in the multiply connected channels formed by the gap between two corrugated plates (see Fig. 1): the crossing flow of small sub-streams following the furrows of the first and the second plate respectively over the whole width of the corrugation pattern dominating at lower inclination angles, and the longitudinal wavy flow between two vertical rows of contact points, prevailing at high  $\phi$  angles.

The limiting case, i.e.  $\phi = 0$ , is the straight longitudinal flow in a number of parallel channels of sinusoidal cross-section (see Fig. 2, top), where the corrugations of the two plates are phase shifted by  $\pi$  so that the plates have line contact along the crests. If the corrugations are in phase, the plates have no contact and the cross-section is a long 'rectangle' with the longer sides sinusoidally waved (Fig. 2, bottom). The latter is mechanically unstable and would require additional constructive measures to prevent the walls from bending under differential pressure. To calculate the pressure drop in this limiting case, one can use the theoretical law of Poiseuille for laminar flow and the semi-empirical law of Prandtl, or any equivalent empirical approximation of it, for turbulent flow:

$$\xi_0 = \frac{B_0}{\text{Re}} \quad \text{Re} < 2000 \text{ (laminar, Poiseuille)} \quad (6)$$

(sin  $\varphi = 0$ ,  $\varphi = 0^\circ$ , straight longitudinal flow)

$$\xi_0 = (1.8 \lg \text{Re} - 1.5)^{-2} \quad \text{Re} \geq 2000 \text{ (turbulent, Konakov)} \quad (7)$$

The constant  $B_0 = \xi_0 \cdot \text{Re}$  depends on the shape of the cross-section; thus  $B_0 = 64$  for a circular tube. Focke et al. [6] have undertaken a numerical calculation to obtain  $B_0$  for the ducts of sine cross-section (Fig. 2, top) and obtained (Eq. (A3) in [6])  $B_{0,\pi} = 53.39$  (which is only valid for  $\Lambda/\hat{a} = 4$ ). Numerical values for other values of  $\Lambda/\hat{a}$ , as well as for the other limit  $B_{0,0}$ , are not known to date, although one might expect a value of magnitude in the order of 90 (the long rectangular cross-section would give  $B_0 = 96$ ). For practical applications, a mean value between these two is recommended for use in Eq. (6). That for a circular tube may be chosen since no better calculations are available, hence:

$$B_0 = 64 \quad (8)$$

For turbulent flow Prandtl's well-known semi-empirical law, i.e.  $1/\sqrt{\xi} = 2 \lg(\text{Re}\sqrt{\xi}) - 0.8$ , implicit in  $\xi$ , may be very well approximated by an explicit expression of the type  $1/\sqrt{\xi} = (2-n) \lg \text{Re} + \text{const.}$ , where the 'constant' is  $\lg(\xi \cdot \text{Re}^n) - 0.8$ . Konakov's equation [Eq. (7)] is one of the simplest, and best, of these approximations. It is to be recommended for turbulent pipe flow in place of the similar Filonenko equation, i.e.  $1/\sqrt{\xi} = 1.82 \lg \text{Re} - 1.64$ , in the next edition of *VDI-Wärmeatlas*.

The other limiting case, i.e.  $\varphi = \pi/2 (= 90^\circ)$ , is the longitudinal wavy flow in a duct of rectangular cross-section. In this case, the shapes shown as cross-sections in Fig. 2 are longitudinal sections. If the corrugations were phase shifted by  $\pi$  so that the plates would have line contacts along the crests, the flow would be blocked [ $\xi_{1,\pi} \rightarrow \infty$ ]. If the corrugations are in phase, the plates have no contact (Fig. 2, bottom) and the wavy duct has a friction factor  $\xi_{1,0}$ , i.e. much larger than for a straight duct. It is known that when flow separation occurs at  $\text{Re} > 20$ , vortices rotate in the vicinity of the outer extrema of the duct walls and the main flow follows a sinusoidal path with the same wavelength, but with a much smaller amplitude. Focke et al. [6] correlated their experimental data for this case as

$$\xi_{1,0} = \frac{B_1}{\text{Re}} + C_1 \quad \text{Re} < 2000 \text{ (laminar, with vortices)} \quad (9)$$

(sin  $\varphi = 1$ ,  $\varphi = 90^\circ$ , wavy longitudinal flow)

$$\xi_{1,0} = \frac{K_1}{\text{Re}^n} \quad \text{Re} \geq 2000 \text{ (fully turbulent)} \quad (10)$$

The constants in Ref. [6] were given for  $\xi_e$  and  $\text{Re}_e$  with  $d_e$  as the characteristic length and hence have to be recalculated here (with  $\Phi = 1.464$  as given in Ref. [6] for

the plates used with  $\Lambda = 10$  mm and  $\hat{a} = 2.5$  mm). Thus with  $B_{1e} = 1280$ ,  $C_{1e} = 5.63$ ,  $K_{1e} = 63.8$ ,  $n = 0.289$ , from Eqs. (14,15) in Ref. [6], one obtains:  $B_1 = B_{1e}/\Phi^2$ ,  $C_1 = C_{1e}/\Phi$ ,  $K_1 = K_{1e}/\Phi^{1+n}$ , i.e.  $B_1 = 597$ ,  $C_1 = 3.85$ ,  $K_1 = 39$ , and  $n = 0.289$ .

The critical Reynolds number (with  $d_e$ ) was given as  $\text{Re}_e = 3000$  in Ref. [6], comparable to  $\text{Re} = 2049$  rounded off in Eqs. (9,10) to 2000. These empirical equations are only valid for the geometrical parameters used in Ref. [6], i.e.  $\Lambda/\hat{a} = 4$ . They will certainly depend on  $\hat{a}/\Lambda$ , as may readily be seen from the fact that for  $\hat{a}/\Lambda \rightarrow 0$ , the straight rectangular duct would have  $B_1 = 96$ ,  $C_1 = 0$  and Eq. (7) for turbulent flow. The friction factor  $\xi_1$  will certainly depend very sensitively on slight changes in phase between the two plates, and on slight changes in the plate distance caused by pressure differences. With the present state of knowledge, the calculation of  $\xi_{1,0}$  from Eqs. (9,10) can only be regarded as a rough estimate and will always be rather uncertain. In practice, the constants  $B_1$ ,  $C_1$ ,  $K_1$  and  $n$  might be used as fitting parameters if experimental data are available.

The range of inclination angles between these two limits, i.e.  $0^\circ < \varphi < 90^\circ$ , may be modelled in the following way. The flow path along the furrows relative to the vertical increases proportional to  $1/\cos \varphi$ , and hence the Reynolds-dependent friction factor  $\xi_0$  has to be replaced by  $\xi_0/\cos \varphi$ . Additional friction losses occur due to flow reversal at the edges of the corrugation pattern and to crossing of the substreams. These two effects may be taken approximately into account by constant friction coefficients multiplied by the number of flow reversals, or the number of crossing points, respectively.

The number of flow reversals (or Back turns) is:

$$n_b = \frac{L_p}{d_h} \cdot \frac{d_h}{B} \cdot \tan \varphi \quad (11)$$

where  $B$  is the width of the corrugation pattern (see Fig. 1). The number  $n_b$  is thus proportional to  $L_p/d_h$ , so that the additional friction due to back turning of the flow may be simply added to  $\xi_0/\cos \varphi$  as

$$\xi_b = b \tan \varphi \quad (12)$$

where

$$b = \zeta_b \frac{d_h}{B} \quad (13)$$

The number of crossing points in a vertical line is:

$$n_c = \frac{L_p}{d_h} \cdot \frac{2d_h}{\Lambda} \cdot \sin \varphi \quad (14)$$

where  $\Lambda$  is the wavelength of the corrugation pattern (see Fig. 1). The number  $n_c$  is also proportional to  $L_p/d_h$ , so that the additional friction due to crossing may be added to  $\xi_0/\cos \varphi$  (and  $\xi_b$ ) too, as

$$\xi_c = c \sin \varphi \quad (15)$$

where

$$c = \xi_c \frac{2d_h}{\Lambda} \quad (16)$$

The total friction factor for crossing flow is therefore given by

$$\xi_{\text{crossing}} = b \tan \varphi + c \sin \varphi + \xi_0(\text{Re})/\cos \varphi \quad (17)$$

The corresponding friction factor for longitudinal wavy flow,  $\xi_1(\text{Re})$ , has to be somewhere between  $\xi_{1,0}(\text{Re})$  from Eqs. (9,10) and  $\xi_{1,\pi} (= \infty)$  and may be taken as  $\xi_1 = a \cdot \xi_{1,0}(\text{Re})$  with the factor  $a \geq 1$ . The flow rates of the two kinds of flow, driven by a common pressure gradient, are proportional to their respective cross-sectional fractions:  $\cos \varphi$  for the crossing flow and  $(1 - \cos \varphi)$  for the longitudinal wavy flow. To a first approximation, they are inversely proportional to the square roots of their respective friction factors, which leads to the relatively simply model equation for  $\xi = f(\varphi, \xi_0(\text{Re}), \xi_1(\text{Re}), b, c)$  with  $\xi_1(\text{Re}) \approx a \cdot \xi_{1,0}(\text{Re})$  as:

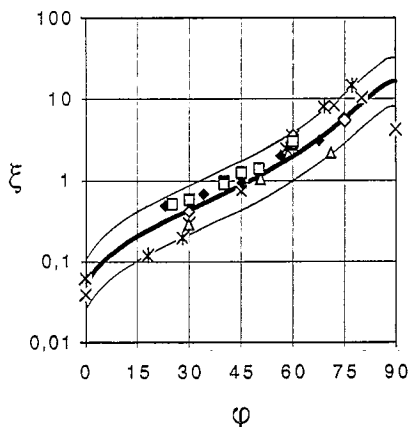


Fig. 3. Effect of the corrugation inclination angle  $\varphi$  on the pressure drop in plate heat exchangers. The friction factor  $\xi(\text{Re} = 2000, \varphi)$  as a function of corrugation inclination angle  $\varphi$  is as follows: (open diamond): Okada et al. [4] (1972): model plates:  $\varphi = 30^\circ, 45^\circ, 60^\circ, 75^\circ$  (here  $\xi = \xi_{\text{model}}(45^\circ) \cdot \Delta p(\varphi)/\Delta p(45^\circ)$ ,  $\xi$  could not be calculated from  $\Delta p$  as in Ref. [4]); (cross): Focke et al. [6] (1985): model plates:  $\varphi = 0^\circ, 30^\circ, 45^\circ, 60^\circ, 72^\circ, 80^\circ, 90^\circ$ ; (star) Gaiser [7] (1990): model plates:  $\varphi = 18^\circ, 28^\circ, 45^\circ, 58^\circ, 69^\circ, 77^\circ$ ; (triangle): Bassiouny [9] (1985): industrial plates (Schmidt, Bretten):  $\varphi = 29.75^\circ, (29.75^\circ \text{ and } 71^\circ), 71^\circ$ ; (square): Bond [8] (1981): diagram for industrial plates:  $\varphi = 25^\circ, 30^\circ, 40^\circ, 45^\circ, 60^\circ$ , and HEDH [3] (Taborek, 1988): diagram for industrial plates:  $\varphi = 30^\circ, 40^\circ, 50^\circ, 60^\circ$ ; (filled diamond): Heavner et al. [10] (1993): industrial plates (APV):  $\varphi = 23^\circ, (23^\circ \text{ and } 45^\circ), 45^\circ, (23^\circ \text{ and } 90^\circ), (45^\circ \text{ and } 90^\circ)$ . Curves: model equation (18) for  $\xi(\varphi, \text{Re})$  with the friction parameters ('standard set')  $(a, b, c) = (3.8, 0.18, 0.36)$ : upper curve,  $2 \cdot \xi$ ; lower curve,  $0.5 \cdot \xi$ .

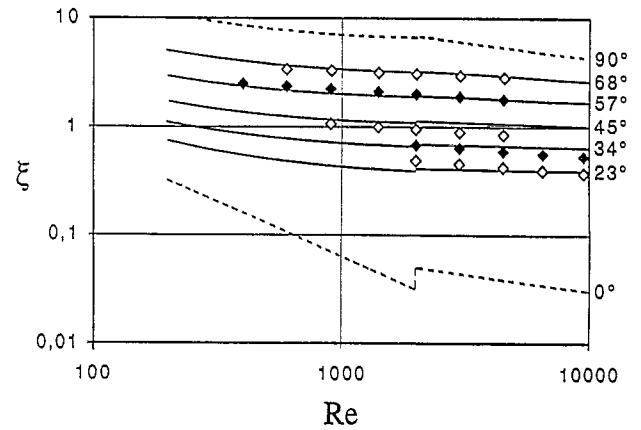


Fig. 4. Plots of the friction factor  $\xi$  versus Reynolds number  $\text{Re}$  with the inclination angle  $\varphi$  as a parameter. Curves calculated from the model equation (18) with  $(a, b, c)$  with  $(1.6, 0.40, 0.36)$ . Symbols: empirical correlations by Heavner et al. (1993) representing their data for technical plates (the values for  $\text{Re} = 2000$  are also shown in Fig. 3 as full diamonds).

$$\frac{1}{\sqrt{\xi}} = \frac{\cos \varphi}{\sqrt{b \tan \varphi + c \sin \varphi + \xi_0(\text{Re})/\cos \varphi}} + \frac{1 - \cos \varphi}{\sqrt{\xi_1(\text{Re})}} \quad (18)$$

Fig. 3 shows a comparison of experimentally obtained friction factors for a constant Reynolds number of 2000 (turbulent flow in nearly all cases) as taken from seven different sources with curves calculated from Eq. (18) using Eqs. (6,7) for  $\xi_0(\text{Re})$  and Eqs. (9,10) for  $\xi_1(\text{Re})$ , while the friction parameters  $a, b$  and  $c$  have been used to fit the data. From these data it can be seen that a variation of the inclination angle  $\varphi$  from  $0^\circ$  to about  $80^\circ$  results in a change in the pressure drop over about 2.5 decades, i.e. a factor of 300 ( $\approx 10^{2.5}$ ). Focke's experimental data for  $90^\circ$ , where the corrugation patterns of the two plates are exactly in phase, are considerably lower than the maximum. The curve from the model equation does not show this behaviour because  $\xi_1$  in the model equation cannot necessarily be identified with this special case, i.e.  $\xi_{1,0}$ . To fit the data over the range of inclination angles from  $0^\circ$  to  $80^\circ$ , a ratio of  $\xi_1$  to  $\xi_{1,0}$  (i.e. the parameter  $a$ ) of about 3.8 had to be chosen. The choice of  $a$ , however, does not significantly change the values of  $\xi$  for angles below  $70^\circ$ . With the exception of the special case of  $90^\circ$ , the model gives the correct trend for  $\xi(\varphi)$ . The relatively large individual deviation — the thinner lines show one-half and twice the values, respectively, of the mean correlation — are certainly due to the fact that the ratio of the corrugation parameters  $\Lambda/\hat{a}$  (which was 3.56, 4 and 5 for the model plates of Gaiser, Focke and Okada, respectively) will probably have been about twice as large as for the industrial plates used in the other investigations [3,8–10]. Only one source, i.e. Ref. [9], gives values of  $\hat{a}$  and  $\Lambda$  of 1.8 mm and 13.78 mm, respectively, i.e.  $\Lambda/\hat{a} = 7.66$ . Since the friction

parameters  $a$ ,  $b$  and  $c$  will clearly depend on the individual geometrical data for the corrugation patterns [see Eqs. (13), (16) and the text following Eqs. (9,10)], a fit to individual sets of data may lead to better agreement. As an example, Fig. 4 shows a comparison between the curves from Eq. (18) and the friction factors  $\xi$  obtained from empirical correlations of the type  $f = K/Re^n$  by Heavner et al. [10], representing their data for industrial plates (the constants  $K$  and  $n$  for each angle  $\varphi$  from Ref. [10] are also given in Table 1, second and third columns. The authors used corrugations with  $\varphi = 23^\circ$ ,  $45^\circ$  and  $90^\circ$ , the angles labelled  $34^\circ$ ,  $57^\circ$  and  $68^\circ$  being obtained as the arithmetic mean of the combinations ( $23^\circ$  and  $45^\circ$ ), ( $23^\circ$  and  $90^\circ$ ) and ( $45^\circ$  and  $90^\circ$ ). Measurements with ( $90^\circ$  and  $90^\circ$ ) were not reported. Flow channels for such combinations would be mechanically unstable due to the lack of contact points between the corrugations. The set of friction parameters ( $a$ ,  $b$ ,  $c$ ) = (1.6, 0.40, 0.36) used in this individual comparison employs the same value for  $c$  as the overall comparison of  $\xi(\varphi)$  for  $Re = 2000$  in Fig. 3 [the standard set of parameters ( $a$ ,  $b$ ,  $c$ )], while the parameter  $a$  has been decreased from 3.8 to 1.6 and  $b$  has been increased from 0.18 to 0.40<sup>1</sup>. The individual

Table 1

Constants for the empirical equations by Heavner et al. (1993) [10]:  $K$ ,  $n$ ,  $c_n$ ,  $m$  as given in Ref. [10];  $q$ ,  $c_x$ ,  $c_q$  calculated from the following equations: Heavner et al.:  $f = K/Re^n$ ;  $Nu^* = c_n Re^m$ ;  $Nu^* = Nu/[Pr^{1/3}(\eta/\eta_w)^{1/6}]$ . Eq. (28):  $Nu^* = c_q[\xi \cdot Re^2 \sin(2\varphi)]^q$ ;  $q = m/(2-n)$ .  $c_x = (4K/1.172) \sin(2\varphi)$ ;  $c_q = c_n/(c_x^q)$

| $\varphi$ (°) | $K$   | $n$   | $c_n$ | $m$   | $q$                | $c_x$ | $c_q$              |
|---------------|-------|-------|-------|-------|--------------------|-------|--------------------|
| 67.5          | 1.715 | 0.084 | 0.278 | 0.683 | 0.356              | 4.139 | 0.168              |
| 56.5          | 1.645 | 0.135 | 0.308 | 0.667 | 0.358              | 5.168 | 0.171              |
| 45            | 0.810 | 0.141 | 0.195 | 0.692 | 0.372              | 2.765 | 0.134              |
| 34            | 0.649 | 0.156 | 0.118 | 0.720 | 0.390              | 2.054 | 0.089              |
| 23            | 0.571 | 0.181 | 0.089 | 0.718 | 0.395              | 1.402 | 0.078              |
|               |       |       |       |       | 0.374 <sup>a</sup> |       | 0.122 <sup>b</sup> |

<sup>a</sup> Arithmetic mean value.

<sup>b</sup> Geometric mean value.

### Note added in proof

My decision to divide the values of  $K$  from Heavner et al. [10] in Table 1 by the factor 1.172 (see Eq. for  $c_x$  in Table 1 and the text at the end of section 2) was essentially confirmed in the meantime by Richard L. Heavner, who kindly sent a list of correct values of these coefficients, which indeed are lower than the ones given in [10] by about  $17 \pm 2\%$ :

| $\varphi$ | wrong | correct |
|-----------|-------|---------|
| 67.5°     | 1.715 | 1.458   |
| 56.5°     | 1.645 | 1.441   |
| 45°       | 0.810 | 0.687   |
| 34°       | 0.649 | 0.545   |
| 23°       | 0.571 | 0.490   |

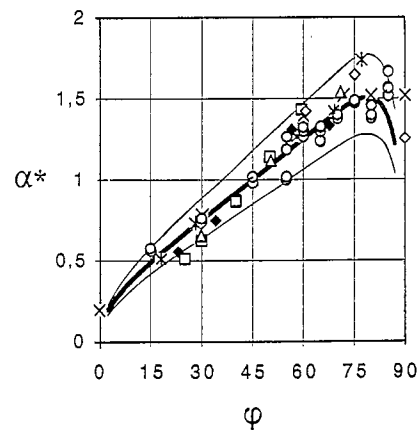


Fig. 5. Effect of the corrugation inclination angle  $\varphi$  on the heat transfer in plate heat exchangers,  $\alpha^* = \alpha(\varphi)/\alpha(45^\circ)$ , employing a normalized heat-transfer coefficient at  $Re = 2000$ . Symbols as in Fig. 3, and (circles): Rosenblad and Kullendorff [5] (1975): (mass-transfer data, small model plate,  $Re = 1880$ )  $\varphi = 15^\circ$ ,  $30^\circ$ ,  $45^\circ$ ,  $55^\circ$ ,  $60^\circ$ ,  $65^\circ$ ,  $70^\circ$ ,  $75^\circ$ ,  $80^\circ$ ,  $85^\circ$ . Curves: generalized L  v  que equation (19)  $\pm 20\%$ , with the standard set of friction parameters ( $a$ ,  $b$ ,  $c$ ) used for  $\xi$  from Eq. (18) as in Fig. 3.

empirical correlations in Ref. [10] need two parameters ( $K$ ,  $n$ ) for each of the five angles, i.e. a total of 10 parameters, while the new model equation needs only a total number of three friction parameters ( $a$ ,  $b$ ,  $c$ ) for the set of five curves, and furthermore allows for easy interpolation or even extrapolation for other inclination angles.

### 3. Heat or mass transfer

Fig. 5 shows the corresponding heat- or mass-transfer data taken from the same seven sources as used in Fig. 3 for  $Re = 2000$ , with the mass transfer data (at  $Re = 1880$ ) of Rosenblad and Kullendorff [5] added (these authors did not measure the pressure drop). In an attempt to eliminate the effects of other parameters, the values are shown in a normalized manner as  $\alpha^* = \alpha(\varphi)/\alpha(45^\circ) = Nu(\varphi)/Nu(45^\circ)$  or  $= j(\varphi)/j(45^\circ)$ , where the corresponding ratio of the mass-transfer coefficients  $\beta(\varphi)/\beta(45^\circ)$  is also included. The data from all the sources mentioned show essentially the same behaviour, with an increase in heat transfer from a value of about

<sup>1</sup> It should be mentioned that the empirical correlations [10] given in Table 1 result in (Fanning) friction factors  $f$  which are 17.2% higher than the corresponding lines through the data (see Ref. [10], in Fig. 3). The possible reason for this systematic discrepancy between the figure and the table might be the effect of not dividing the values in the table by the area enhancement factor  $\Phi$ , leading to a friction factor defined with  $d_e$  according to Eq. (5) in place of  $d_h$ . The value of  $\Phi$  is not given in Ref. [10], but 1.172 might well be a reasonable value for  $\Phi$  for an industrial plate. The values shown as symbols in Fig. 4 (and in Fig. 3) have been calculated from the empirical correlations for  $f$  (with  $\xi = 4 \cdot f$ ) of Heavner et al. [10] divided by 1.172 in order to represent the data correctly.

$\alpha^* \approx 0.25$  at  $\varphi = 0^\circ$  to a maximum of about 1.7 at  $80^\circ$ . The ratio of the maximum to the minimum heat transfer is  $\alpha_{\max}/\alpha_{\min} \approx 7$ . Compared to the ratio of the maximum to minimum momentum transfer of 2.5 orders of magnitude, or  $\xi_{\max}/\xi_{\min} = 10^{2.5} \approx 300$ , these ratios are obviously related to each other by  $\alpha_{\max}/\alpha_{\min} = (\xi_{\max}/\xi_{\min})^{1/3}$ , i.e. (300)<sup>1/3</sup> = 6.7.

The curves shown in Fig. 5 have been calculated from a purely theoretical equation, which may be called the generalized L ev eque equation [11,12], with  $\xi(\text{Re}, \varphi)$  from Eq. (18) and  $(a, b, c)$  as used in Fig. 3:

$$\text{Nu} = 0.40377(\xi \cdot \text{Re}^2 \cdot \text{Pr} \cdot d/L)^{1/3} \quad (19)$$

(the constant is  $0.40377454 \dots = 3^{4/3}/[4 \cdot \Gamma(1/3)]$ , where  $\Gamma(x) = \int_0^\infty e^{-t} \cdot t^{x-1} dt$  is the Gamma function with  $\Gamma(x=1/3) = 2.6789385 \dots$ ). The length  $L$  in this case is taken as the distance between two crossings (see Fig. 1):

$$L = \Lambda/\sin(2\varphi) \quad d/L = (d_h/\Lambda) \cdot \sin(2\varphi) \quad (20)$$

The L ev eque equation is a well known equation for the heat transfer through developing thermal boundary layers in a hydrodynamically developed laminar duct flow. It had also been used for laminar flow and for  $\varphi = 0^\circ$  alone, with  $L = L_p$  (the whole plate length) by Focke et al. [6].

For a circular tube, with  $(\xi \cdot \text{Re})_{\text{laminar tube flow}} = 64$ , Eq. (19) takes the form which is found in most textbooks on heat transfer, i.e.

$$\text{Nu} = 1.615(\text{Re} \cdot \text{Pr} \cdot d/L)^{1/3} \quad (21)$$

To date, it does not seem to have been really applied to turbulent flow, although there is no reason to restrict its application to the laminar range. It has, in fact, been mentioned in a paper on ‘The Historical Development and Present State of the Scientific Theory of Heat Transfer’ published in German in 1971 by Schl under [12], p. 8:

“... und es d urft vermutlich nur einen einzigen Fall des turbulenten W arme berganges geben, f ur den man aus den klassischen Differentialgleichungen der viskosen Str omung eine Gleichung\*) herleiten kann, die an keine irgendwie geartete Modellvorstellung  uber den Mechanismus der turbulenten Str omung gebunden ist und daher als streng im klassischen Sinne gelten darf. Sie gilt jedoch nur f ur extrem kurze beheizte Rohrstrecken, die von ausgebildeter turbulenter Str omung durchsp ult werden, und ist daher mehr von akademischer als von praktischer Bedeutung.” (“... and there might probably be one single case of turbulent heat transfer only, for which an equation\* can be derived from the classical differential equations for viscous flow which are bound to no modelling concept, whatsoever, on the mechanism for turbulent flow, and therefore may be taken as rigorous in the classical sense. It is only valid, however, for extremely short heated lengths of tube with a developed turbulent flow, and therefore it is more of an

academic than of a practical value.”) Eq. (19) is given in the footnote\* on p. 8 of Ref. [12]. As  $L$  has been taken here as the distance between two crossings, which tends to infinity for the limiting cases  $\varphi = 0^\circ$  and  $\varphi = 90^\circ$ , the formula cannot be applied in these two cases.

Obviously, this theoretical equation (19) [with Eq. (20)], combined with the model equation (18) or used directly with the measured friction factors  $\xi(\varphi)$ , agrees very well with the experimentally observed variation of heat- or mass-transfer coefficients with the corrugation inclination angle. The upper and lower thinner lines in Fig. 5 are the theoretical result  $\pm 20\%$ . The good agreement between the theoretical prediction and experimental observation, however, may be partly due to the normalization with respect to the corresponding data for  $\varphi = 45^\circ$ , which has been used in order to eliminate the effects of other parameters.

To check whether the effects of other variables such as the flow rate (Re) or length scales of the corrugation will also be reasonably represented by this strikingly simple theory, the comparison shown in Fig. 5 is not sufficient. Fig. 6 therefore shows a plot of the exponents  $m$  for empirical equations of the type (see Table 1, columns 4 and 5 for values of  $c_n$  and  $m$  taken from Ref. [10]):

$$\text{Nu}^* = c_n \cdot \text{Re}^m \quad (22)$$

which have been used by many authors to correlate their experimental data in the turbulent range.  $\text{Nu}^*$  is a group containing the Nusselt number divided by  $\text{Pr}^{1/3}$

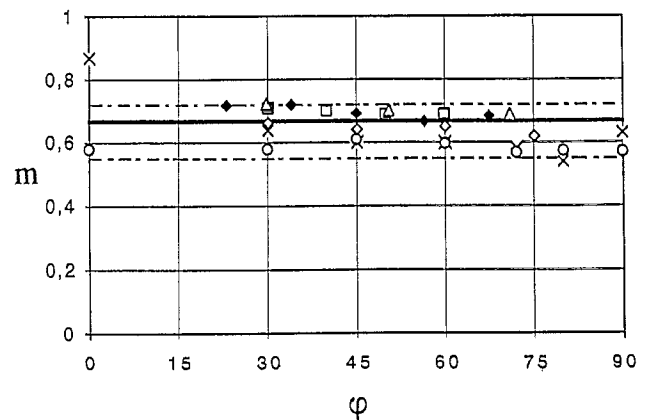


Fig. 6. The exponents  $m$  in  $\text{Nu}^* = c_n \cdot \text{Re}^m$  (or  $\text{Sh}^*$ ) as a function of the inclination angle  $\varphi$ . Broken lines:  $m = 0.72$ ,  $m = 0.55$ , Full line:  $m = 2/3$  (L ev eque theory for  $\xi = \text{const.}$ ). The points indicated are as follows: (cross): Focke et al. [6] (1985): model plates:  $\varphi = 0^\circ, 30^\circ, 45^\circ, 60^\circ, 72^\circ, 80^\circ, 90^\circ$ ; (circle) theoretical values of  $m = (2 - n)/3$  from generalized L ev eque equation, where  $n$  is the exponent in  $\xi = K/\text{Re}^n$  taken from Focke et al. (1985); (open diamond): Okada et al. [4] (1972): model plates:  $\varphi = 30^\circ, 45^\circ, 60^\circ, 75^\circ$ ; (triangle) Bassiouny [9] (1985): industrial plates (Schmidt, Bretten):  $\varphi = 29.75^\circ, (29.75^\circ \text{ and } 71^\circ), 71^\circ$ ; (square): HEDH [3] (Taborek, 1988): diagram for industrial plates:  $\varphi = 30^\circ, 40^\circ, 50^\circ, 60^\circ$ ; (filled diamond): Heavner et al. [10] (1993): industrial plates (APV):  $\varphi = 23^\circ, (23^\circ \text{ and } 45^\circ), 45^\circ, (23^\circ \text{ and } 90^\circ), (45^\circ \text{ and } 90^\circ)$ .

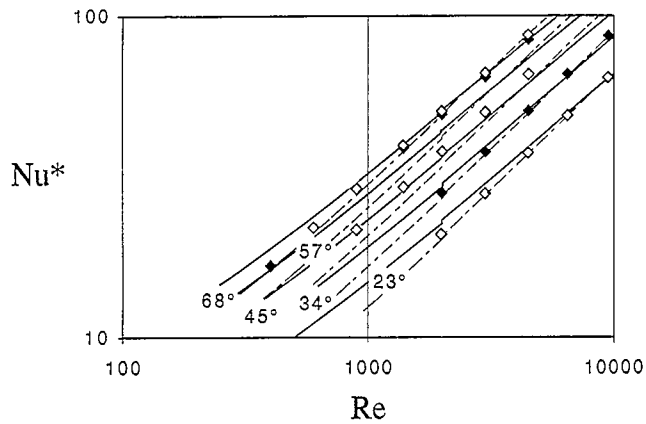


Fig. 7.  $Nu^* = Nu \cdot Pr^{-(1/3)}(\eta/\eta_w)^{-(1/6)}$  versus  $Re$  with the inclination angle  $\varphi$  as a parameter. Full lines calculated from the theoretical L ev eque equation (19) with Eq. (20), and  $\xi$  from Eq. (18) using the standard set of friction parameters  $(a, b, c) = (3.8, 0.18, 0.36)$  and  $(d_h/\Lambda) = 0.21$ . Symbols: empirical correlations by Heavner et al. [10] (1993) representing their data for technical plates (see Table 1); dotted lines: calculated from Eq. (28) (based on the L ev eque analogy, adapted to the experimental results) with  $\xi$  as above.

[3,5,6,8,10] or by  $Pr^{0.4}$  [4,9] and, partly, by a viscosity ratio correction term  $(\eta/\eta_w)^{0.17}$  [3,8,10]. [Some of the authors used the Colburn  $j$ -factor ( $j = Nu \cdot Re^{-1} \cdot Pr^{-(1/3)}$ ,  $j = c_j \cdot Re^{-p}$ ) or related groups in place of  $Nu$ ; in these cases the exponent  $m$  is obtained as  $m = 1 - p$ ]. All the  $m$  values which were taken, as far as possible, from the same sources as used in the previous figures, were found to be between 0.55 and 0.72 (shown by the broken horizontal lines in Fig. 6) with the exception of a single much higher value  $m = 0.868$  ( $= 1 - 0.132$ ) obtained for straight longitudinal turbulent flow ( $\varphi = 0^\circ$ ) by analogy to a tube flow equation in the paper by Focke et al. [6]. The circles indicate values  $m_L = (2 - n)/3$ , with  $n$  being the exponents in the friction factor formula of the same type as Eq. (10) taken from the empirical correlations of Focke et al. in the turbulent range. These values of  $m_L$  would be the theoretical value of  $m$  which follow from the generalized L ev eque equation. Except for  $\varphi = 0^\circ$ , they are indeed not far away from the empirically obtained values of  $m$  by the same authors (shown as the crosses X in Fig. 6). The full horizontal line is  $m = 2/3$ , i.e. the L ev eque exponent for a friction factor which does not depend on  $Re$  ( $m_L$  for  $n = 0$ ). The average value of all the exponents is not far from  $2/3$ . Values above  $2/3$ , which would only be consistent with the L ev eque theory for negative values of  $n$  (or friction factors increasing with  $Re$ , which may indeed be sometimes found in small ranges of Reynolds numbers between laminar and turbulent flow) are mainly found for technical heat exchanger plates. There seems to be a slight trend to larger

values of  $m$  with lower inclination angles  $\varphi$ . This might be interpreted as the start of a transition from a thermally developing to a more and more developed heat transfer, finally leading to higher exponents between 0.8 and 0.9 for turbulent flow in straight ducts ( $\varphi = 0^\circ$ ).

A more direct comparison between theory and experiment is shown in Fig. 7. Curves obtained from Eqs. (19) and (20) for  $Nu^* = Nu/Pr^{1/3}$  (the full lines), with the friction factors  $\xi$  as calculated from Eq. (18) using the friction parameters  $(a, b, c)$  as in Fig. 3, are compared with correlation equations (the various symbols) representing the experimental data of Heavner et al. [10] for  $Nu^* = Nu/[Pr^{1/3}(\eta/\eta_w)^{0.17}]$  as functions of the Reynolds number with the inclination angle as a parameter (see Table 1, columns 4 and 5 for the values of  $c_n$  and  $m$  from Ref. [10]). As the geometrical details of the plates used by these authors were not given in Ref. [10], the parameter  $d_h/\Lambda$  in Eq. (20) has been used to fit the theoretical curves to the experimental data. The resulting value  $(d_h/\Lambda)_{fit} = 0.21$  is probably lower than the actual geometric one. A typical value of  $d_h/\Lambda$  for technical plates may be obtained from Bassiouny [9] for example: thus with  $\Lambda/\hat{a} = 7.66$ ,  $\Phi = 1.16$ ,  $d_h/\Lambda = 0.45$  is obtained. Assuming that Heavner's plates had similar geometrical parameters, the ratio  $(0.45/0.21)^{1/3} \approx 1.29$  would mean that the theoretical prediction (without fitting) might be about 30% higher in this case than the experimental result. Simple application of the L ev eque theory does indeed give the correct order of magnitude for the heat- or mass-transfer coefficients in chevron-type plate heat exchangers. (The dotted lines in this figure have been calculated from Eq. (28) as explained below in Section 5.)

#### 4. On the analogy between heat, mass and momentum transfer

The generalized L ev eque equation (19) may be seen as a special form of the analogy between heat, mass and momentum transfer. The classical analogy has been established for fully developed temperature, concentration and velocity profiles in turbulent flow by Osborne Reynolds, Ludwig Prandtl and — following their routes — by many others. In general, the analogy in its various forms provides practically useful interrelations between the transport phenomena.

For ideal gases, the Reynolds analogy predicts a linear relationship between the heat- and the mass-transfer coefficient and the friction factor:

$$\frac{Nu}{Re \cdot Pr} = \frac{Sh}{Re \cdot Sc} = \frac{\xi}{8} \quad (Pr \approx Sc \approx 1) \quad (23)$$

The Prandtl analogy in its original or more refined modern versions shows that this simple proportionality [for  $\text{Pr}(\text{Sc}) \neq 1$ ] has to be replaced by expressions such as:

$$\frac{\text{Nu}}{\text{Re} \cdot \text{Pr}} = \frac{(\xi/8)}{1 + c\sqrt{(\xi/8)(\text{Pr}^n - 1)}}; \quad \frac{\text{Sh}}{\text{Re} \cdot \text{Sc}} = \frac{(\xi/8)}{1 + c\sqrt{(\xi/8)(\text{Sc}^n - 1)}} \quad (24)$$

The linear proportionality between  $\text{Nu}$  ( $\text{Sh}$ ) and  $\xi$  is therefore replaced by a proportionality to  $\xi^b$ , with the exponent varying between  $b = 1$  [for  $\text{Pr}(\text{Sc}) = 1$ ] and  $b = 0.5$  [for  $\text{Pr}(\text{Sc}) \rightarrow \infty$ ].

From the preceding sections [see Eq. (19)], it may follow that for the case of developing thermal (or diffusional) boundary layers in a developed velocity profile, the interrelation between  $\text{Nu}$  ( $\text{Sh}$ ) and  $\xi$  may be even weaker, i.e.  $b = 0.333$ . It is suggested that this special case of the interrelation between heat, mass and momentum transfer be called the L ev eque analogy:

$$\frac{\text{Nu}}{\text{Pr}^{1/3}} = \frac{\text{Sh}}{\text{Sc}^{1/3}} = 0.404 \cdot (d/L)^{1/3} \cdot (\xi \cdot \text{Re}^2)^{1/3} \quad (25)$$

This may be easily adapted to correlate experimental data for plate heat exchangers by replacing the theoretical constant [including the geometrical parameter  $d_h/\Lambda$  from Eq. (20)] and the theoretical exponent  $1/3$  if necessary by appropriate values obtained from experimental results.

## 5. Practical application of the L ev eque analogy

The most striking consequence of the fact that the ‘L ev eque analogy’ applies so nicely to plate heat exchangers may be seen from the dependency of the heat- and mass-transfer coefficients on the product  $\xi \cdot \text{Re}^2$ , which is directly proportional to the pressure drop  $\Delta p$  [see Eq. (1)]:

$$\xi \cdot \text{Re}^2 = \frac{2\Delta p d_h^3 \rho}{L_p \eta^2} \quad (26)$$

This indicates that the heat- and mass-transfer coefficients are independent (or virtually independent) of the individual values of the flow rate ( $\text{Re}$ ) and inclination angle  $\varphi$ . The term  $(d/L)^{1/3}$  in Eq. (20) is proportional to  $[\sin(2\varphi)]^{1/3}$ , which is unity for  $\varphi = 45^\circ$  and deviates from this maximum value by less than 10% over the range of inclination angles from  $25^\circ \leq \varphi \leq 65^\circ$ , resulting in a rather weak individual dependency on  $\varphi$ . A plate heat exchanger with (‘soft’) ‘low phi’ plates (say with  $\varphi = 30^\circ$ ) will have the same heat-transfer coefficient as a one with (‘hard’) ‘high phi’ plates ( $\varphi = 60^\circ$ , for example) if both are operated with the same pressure difference  $\Delta p$ ! The flow rates will differ, however, by

more than a factor of two. So the ‘high phi’ plates, with a given pressure drop, will produce higher numbers of transfer units (NTU) or higher temperature changes. This is a well known fact and the (nearly) ‘universal’ relationship between the heat-transfer coefficient and the pressure drop for plate heat exchangers has been empirically observed and documented, for example, in a figure showing the heat-transfer coefficient  $\alpha$  versus pressure drop  $\Delta p$  for a water-to-water (313 K) application by Cooper and Usher [3] (see Fig. 2 in Section 3.7.10 of their report). This figure, which is said to show an ‘ $\alpha/\Delta p$  curve representative of plates in general, where  $\alpha$  in this case is equal to  $2U$ , thereby incorporating an approximate allowance for metal resistance’, is an essentially straight line in a log–log plot from  $\alpha_{\text{overall}}(\Delta p = 0.1 \text{ bar}) \approx 6300 \text{ W m}^{-2} \text{ K}^{-1}$  via  $\alpha_{\text{overall}}(\Delta p = 1.0 \text{ bar}) \approx 12600 \text{ W m}^{-2} \text{ K}^{-1}$  (water, 313 K) to  $\alpha_{\text{overall}}(\Delta p = 1.6 \text{ bar}) \approx 14500 \text{ W m}^{-2} \text{ K}^{-1}$ . In the form of an equation, this curve may be expressed approximately as ( $10^{0.30} = 2$ ):

$$\alpha_{\text{overall}} \approx 12600 \text{ W m}^{-2} \text{ K}^{-1} \times (\Delta p/1 \text{ bar})^{0.30} \quad (\text{water, 313 K}) \quad (27)$$

(The subscript ‘overall’ here means:  $\alpha_{\text{overall}} = 2/(2/\alpha + (s/\lambda)_{\text{metal}})$ , i.e. this ‘ $\alpha$ ’ is twice the overall heat-transfer coefficient  $U$  as stated by Cooper and Usher [3], see above).

The L ev eque analogy would predict an exponent of 0.333 for  $\alpha$  as a function of  $\Delta p$ . Empirical evidence from various sources with technical plates would lead to a slightly higher exponent (see Figs. 6 and 7). Using the empirical equations of Heavner et al. [10] for the friction factors ( $f = K \cdot \text{Re}^{-n}$ ) and the Nusselt numbers ( $\text{Nu}^* = c_n \cdot \text{Re}^m$ ) respectively (see Table 1), covering inclination angles from  $23^\circ$  to  $68^\circ$ , one obtains an average exponent of  $q = [m/(2-n)]_{\text{average}} = 0.374$  (with maximum deviations of  $-4.7\%$  to  $+5.6\%$ ) in place of  $q = 0.333$  from the direct application of the L ev eque theory. A good semi-empirical equation, representing the heat-transfer data by Heavner et al. [10] together with their data on pressure drop [or with Eq. (18)] is obtained from replacing  $\text{Re}$  in  $\text{Nu}^* = c_n \cdot \text{Re}^m$  by the value obtained from solving the equation  $\xi \cdot \text{Re}^2 \sin(2\varphi) = x = c_x \cdot \text{Re}^{2-n}$  for the Reynolds number on the right-hand side, i.e.  $\text{Re} = (x/c_x)^{1/(2-n)}$ . So, finally, the empirical equations of Heavner et al. are rewritten in the form  $\text{Nu}^* = c_q [\xi \cdot \text{Re}^2 \sin(2\varphi)]^q$ , with the adapted exponents  $q$  and constants  $c_q$  obtained from the corresponding friction factor correlations as listed in Table 1. Taking the arithmetic mean of the five values of  $q$  and the geometric mean of the five constants  $c_q$  (which is the appropriate averaging for a set of power laws), one finally obtains a practically useful semi-empirical equation for heat transfer in technical plates, based on the L ev eque analogy and on experimental evidence:

$$\text{Nu} = 0.122\text{Pr}^{1/3}(\eta/\eta_w)^{1/6} \cdot [\xi \cdot \text{Re}^2 \sin(2\varphi)]^{0.374} \quad (28)$$

This equation when used with the model equation (18) for  $\xi(\text{Re}, \varphi)$  and the standard set of friction parameters  $(a, b, c) = (3.8, 0.18, 0.36)$  in fact represents the heat transfer data by Heavner et al. [10] somewhat better than the original L ev eque equation. This is shown by the dotted curves in Fig. 7.

Eq. (28) may easily be rewritten in terms of  $\Delta p$ , with Eq. (26). Using the physical properties of water at 313 K, as given by Cooper and Usher [3], i.e.  $\rho = 1000 \text{ kg m}^{-3}$ ,  $C_p = 4.2 \times 10^3 \text{ J kg}^{-1} \text{ K}^{-1}$ ,  $\eta = 0.65 \times 10^{-3} \text{ Pa s}$  and  $\lambda = 0.63 \text{ W K}^{-1} \text{ m}^{-1}$ , together with  $L_p = 1 \text{ m}$  (or rather  $\Delta p$  replaced by a pressure gradient  $\Delta p/L_p$  in  $\text{bar m}^{-1}$ ),  $d_h = 4 \text{ mm}$  (the value of  $d_h$  has a weak influence here, with a power of only 0.122) and the property ratio correction  $(\eta/\eta_w)^{1/6}$  put equal to one, finally gives:

$$\alpha_{\text{water}, 313 \text{ K}} = 19\,677[(\Delta p/1 \text{ bar}) \sin(2\varphi)]^{0.374} \text{ W m}^{-2} \text{ K}^{-1} \quad (29)$$

Using angles of  $\varphi = 30^\circ$  and  $60^\circ$  for example [ $\sin(2 \times 30^\circ) = \sin(2 \times 60^\circ) = 0.866$ ], one obtains  $\alpha_{\text{water}, 313 \text{ K}} = 18\,646(\Delta p/1 \text{ bar})^{0.374} \text{ W m}^{-2} \text{ K}^{-1}$  and allowing for a typical stainless-steel wall resistance with a conductivity of  $\lambda_w = 15 \text{ W K}^{-1} \text{ m}^{-1}$  and a wall thickness of  $s_w = 0.75 \text{ mm}$ , i.e.  $(1/20\,000) \text{ m}^2\text{K W}^{-1}$ , gives  $\alpha_{\text{overall}} = 2/[2/\alpha + (s/\lambda)_w]$ :

$$\left. \begin{aligned} \alpha_{\text{overall}}(\Delta p = 0.1 \text{ bar}) &= 6590 \text{ W m}^{-2} \text{ K}^{-1} \\ \alpha_{\text{overall}}(\Delta p = 1.0 \text{ bar}) &= 12\,700 \text{ W m}^{-2} \text{ K}^{-1} \\ \alpha_{\text{overall}}(\Delta p = 1.6 \text{ bar}) &= 14\,300 \text{ W m}^{-2} \text{ K}^{-1} \end{aligned} \right\}$$

[water, 313 K, from Eq. (28)]

which are indeed pretty close to the values of 6300, 12 600 and 14 500  $\text{W m}^{-2} \text{ K}^{-1}$  respectively from the above-mentioned ‘‘ $\alpha/\Delta p$  curve representative of plates in general’’ from the *Heat Exchanger Design Handbook* [3].

The practically important result that heat- and mass-transfer coefficients in plate heat exchangers depend essentially on the pressure gradient (or on the product  $\xi \cdot \text{Re}^2$ ), but not separately on both the friction factor  $\xi(\varphi, \text{Re})$  and the flow rate ( $\text{Re}$ ), seems to date to have been based only on experience. It may now be understood from the application of theory.

## 6. Conclusions

On the basis of present knowledge, Eq. (18) and (28) may be recommended for obtaining the friction factors  $\xi$  and the heat-transfer coefficients  $\alpha$  typically found in technical plate heat exchangers directly as a function of the corrugation inclination angle  $\varphi$ , the Reynolds num-

ber  $\text{Re}$ , or alternatively as a function of the pressure drop ( $\xi \cdot \text{Re}^2$ ) [see Eq. (26)].

More detailed comparison with the original data should be carried out within the near future in order to test and further improve this practically useful design method based on a physically reasonable flow model for  $\xi(\varphi, \text{Re})$  and on a special form of analogy between momentum, heat and mass transfer found from generalizing the L ev eque theory for turbulent flow. The latter idea has been discussed earlier [12] as a more or less academic example of a rigorous theoretical equation that may be applied for turbulent heat transfer. It has been shown, at least for chevron-type plate heat exchangers, that this theory is not only of academic value but is in fact directly applicable for solving practical engineering problems.

## 7. Nomenclature

|                 |   |
|-----------------|---|
| $a, b, c$       | friction parameters in Eq. (18), ‘standard set’: (3.8, 0.18, 0.36), –                     |
| $\hat{a}$       | amplitude of corrugation (see Fig. 1), m  |
| $B$             | width of corrugation pattern (see Fig. 1), m  |
| $B_0, B_1$      | constants in Eq. (6) and (9), –   |
| $c_p, c_q, c_x$ | constants defined in Table 1, –   |
| $C_p$           | specific heat capacity at constant pressure, $\text{J kg}^{-1} \text{ K}^{-1}$            |
| $d_e$           | equivalent diameter, Eq. (5), $d_e = 4\hat{a}$ , m  |
| $d_h$           | hydraulic diameter, Eq. (2), $d_h = 4\hat{a}/\Phi$ , m                                    |
| $f$             | Fanning friction factor, $f = \xi/4$ , –  |
| $j$             | Colburn $j$ -factor, $j = \text{Nu} \cdot \text{Re}^{-1} \cdot \text{Pr}^{-(1/3)}$ , –    |
| $K$             | constant in Eq. (10), –   |
| $L$             | length between two crossing points, Eq. (20), m   |
| $L_p$           | plate length (see Fig. 1), m  |
| $m$             | exponent in Eq. (22), –   |
| $n$             | exponents in Eqs. (10) and (24), numbers, –   |
| $\text{Nu}$     | Nusselt number = $\alpha d_h/\lambda$ , –   |
| $\text{Nu}^*$   | Nusselt group = $\text{Nu} \cdot \text{Pr}^{-(1/3)} \cdot (\eta/\eta_w)^{-(1/6)}$ , –     |
| $\text{Pr}$     | Prandtl number = $\eta C_p/\lambda$ , –   |
| $q$             | exponent in generalized L ev eque analogy (Table 1), –                                    |
| $\text{Re}$     | Reynolds number = $\rho u d_h/\eta$ , –   |
| $s$             | thickness, m  |
| $u$             | flow velocity, $\text{m s}^{-1}$  |
| $U$             | overall heat-transfer coefficient, $\text{W m}^{-2} \text{ K}^{-1}$                       |
| $X$             | corrugation parameter = $2\pi\hat{a}/\Lambda$ , –   |
| $\alpha$        | heat-transfer coefficient, $\text{W m}^{-2} \text{ K}^{-1}$                               |
| $\alpha^*$      | normalized heat- (or mass-) transfer coefficient = $\alpha(\varphi)/\alpha(45^\circ)$ , – |

|           |   |
|-----------|---|
| $\varphi$ | corrugation inclination angle (see Fig. 1),<br>–              |
| $\Phi$    | area enlargement factor = developed<br>area/projected area, – |
| $\eta$    | viscosity, Pa s   |
| $\Lambda$ | wavelength (see Fig. 1), m                                    |
| $\lambda$ | thermal conductivity, $\text{W m}^{-1} \text{K}^{-1}$         |
| $\rho$    | density, $\text{kg m}^{-3}$                                   |
| $\xi$     | friction factor, defined in Eq. (1) = $4f$ , –                |
| $\zeta$   | friction coefficients, Eqs. (13) and (16), –                  |

### Subscripts

|          |   |
|----------|---|
| $0, \pi$ | at the angle $\varphi = 0$ , phase = $\pi$ (between<br>the corrugations of two plates)    |
| 1        | at the angle $\varphi = 90^\circ$ ( $\sin \varphi = 1$ )                                  |
| 1,0      | at the angle $\varphi = 90^\circ$ , phase = 0 (between<br>the corrugations of two plates) |
| b        | back turns, i.e. flow reversals   |
| c        | crossings   |
| e        | defined with $d_e$ , Eq. (5), in place of $d_h$ ,<br>Eq. (1)                              |
| w        | at wall temperature, wall   |

### References

- [1] G. Walker, *Industrial Heat Exchangers: A Basic Guide*, 2nd edn., Hemisphere Publishing Co., Washington/Philadelphia/London, 1990.

- [2] H. Martin, *Heat Exchangers*, Hemisphere Publishing Co., Washington, DC, 1992.
- [3] A. Cooper and J.D. Usher, Plate heat exchangers, in E.U. Schlünder (ed.), *Heat Exchanger Design Handbook*, Hemisphere Publishing Co., Washington, DC, 1983, Vol. 3, Section 3.7; Supplement, 1989.
- [4] K. Okada, M. Ono, T. Tomimura, T. Okuma, H. Konno and S. Ohtani, Design and heat transfer characteristics of new plate heat exchanger, *Heat Transfer—Jpn. Res.*, 1 (1972) 90–95.
- [5] G. Rosenblad and A. Kullendorff, Estimating heat transfer rates from mass transfer studies on plate heat exchanger surfaces, *Wärme Stoffübertrag.*, 8 (1975) 187–191.
- [6] W.W. Focke, J. Zachariades and I. Olivier, The effect of the corrugation angle on the thermohydraulic performance of plate heat exchangers, *Int. J. Heat Mass Transfer*, 28 (1985) 1469–1479.
- [7] G. Gaiser, Stömungs- und Transportvorgänge in gewellten Strukturen, *Dissertation*, Universität Stuttgart, 1990.
- [8] M.P. Bond, Plate heat exchangers for effective heat transfer, *Chem. Eng. (London)*, (April 1981) 162–167.
- [9] M.K. Bassiouny, Experimentelle und theoretische Untersuchungen über Mengenstromverteilung, Druckverlust und Wärmeübergang in Plattenwärmeaustauschern, *Forsch.-Ber. VDI*, Reihe 6, Nr. 181, VDI-Verlag, Dusseldorf, 1985.
- [10] R.L. Heavner, H. Kumar and A.S. Wanniarachchi, Performance of an industrial plate heat exchanger: effect of chevron angle, *AIChE Symp. Ser. No. 295*, Vol. 89, *Heat Transfer*, Am. Inst. Chem. Eng. Atlanta, GA, 1993, pp. 262–267.
- [11] A. Lévêque, Les lois de la transmission de chaleur par convection, *Ann. Mines, Ser. 12, 13* (1928) 201–415.
- [12] E.U. Schlünder, Die wissenschaftliche Theorie der Wärmeübertragung-geschichtliche Entwicklung und heutiger Stand, *DECHEMA-Monogr.*, 65 (1971) 1–18.